

Three-dimensional finite difference time domain modeling of the Earth-ionosphere cavity resonances

Heng Yang and Victor P. Pasko

Communications and Space Sciences Laboratory, Penn State University, University Park, Pennsylvania, USA

Received 24 August 2004; revised 10 January 2005; accepted 18 January 2005; published 15 February 2005.

[1] Comparison of results from a three-dimensional (3-D) finite difference time domain (FDTD) model of Schumann resonances (SR) with a set of classical eigenfrequency and quality factor solutions for laterally uniform spherically symmetric Earth-ionosphere cavity and recent SR observations during solar proton events (SPEs) and X-ray bursts demonstrate the potential and applicability of the FDTD technique for studies of realistic SR problems. **Citation:** Yang, H., and V. P. Pasko (2005), Three-dimensional finite difference time domain modeling of the Earth-ionosphere cavity resonances, *Geophys. Res. Lett.*, 32, L03114, doi:10.1029/2004GL021343.

1. Introduction

[2] Resonance properties of the Earth-ionosphere cavity were predicted by W. O. Schumann in 1952 [Schumann, 1952]. Since then observations of electromagnetic signals in the frequency range 1–500 Hz have become a powerful tool for variety of remote sensing applications [e.g., Williams, 1992; Cummer, 2000; Roldugin et al., 2004], which in recent years included studies of thunderstorm related transient luminous events in the middle atmosphere [e.g., Sato and Fukunishi, 2003].

[3] The FDTD technique [e.g., Taflove and Hagness, 2000] represents one of the simplest and most flexible means for finding electromagnetic solutions in a medium with arbitrary inhomogeneities, and several reports about application of this technique to solution of VLF/ELF propagation problems in the Earth-ionosphere cavity have recently appeared in the literature [e.g., Pasko et al., 1998; Thevenot et al., 1999; Cummer, 2000; Berenger, 2002; Simpson and Taflove, 2002, 2004; Otsuyama et al., 2003].

[4] The purpose of this paper is to provide a comparison of results obtained using a 3-D FDTD model of the Earth-ionosphere cavity with well established solutions of SR problems in order to demonstrate the applicability of FDTD technique for studies of realistic SR problems.

2. Model Formulation

[5] We employ a simplified version of a 3-D FDTD model originally introduced by Yang and Pasko [2003]. A spherical simulation domain is assumed to be confined between two concentric perfectly conducting spheres, with the radius of the inner sphere, corresponding to the Earth surface, set at $R_E = 6370$ km, and with the surface of outer sphere positioned at altitude $h = 100$ km. The 3-D FDTD equations in the spherical coordinates (r, θ, ϕ) are derived

from the Maxwell's equations in a classical manner [Taflove and Hagness, 2000, p. 75]. The singularities at the poles are resolved using integral form of Maxwell's equations. The numbers of cells in r, θ and ϕ directions are 40, 20 and 40, respectively. The cavity is excited by a vertical lightning current with 2.5 km length, which has a linear rise time 500 μ s and exponential fall with time scale 5 ms. The reported results for frequencies <40 Hz are not sensitive to the specifics of the chosen lightning current waveform. The lightning source is positioned near the Earth surface at 0° N, 0° E and a vertical electric field component E_r is monitored at the ground surface by a set of receivers at 18° N 0° E, 36° N 0° E, 54° N 0° E, 72° N 0° E, and 90° N 0° E. The time step Δt is determined by the Courant condition [e.g., Taflove and Hagness, 2000, p. 136]. We report results on first five SR eigenfrequencies f_n and associated Q factors Q_n obtained from modeled E_r power spectrum ($Q_n = f_n/\Delta f_n$, where Δf_n is the full width at half maximum power of the n th mode). For this purpose we employ three different analysis techniques: (1) the fitting of the time domain E_r data with complex polynomials using a Prony's method [Hildebrand, 1956, p. 379; Füllekrug, 1995]; (2) the interpolation of E_r power spectrum data in frequency domain using a Cauchy method [Adve et al., 1997, and references therein]; (3) the least-squares fitting of E_r power spectrum by Lorentzian functions [Sentman, 1987; Heckman et al., 1998; Mushtak and Williams, 2002]. In contrast to real experiments the model FDTD data is high quality, and the analysis using the above three techniques leads to essentially identical results in terms of f_n and Q_n values, with maximum deviations not exceeding 2%. The specific values of Δt and the resolution in frequency domain Δf are shown in Figures 1b and 2a. A factor of two changes in the chosen grid dimensions lead to <0.4% variations in SR frequencies reported in Figures 2a and 3b. Except for the discussion in Sections 3 and 4 related to SPEs and X-ray bursts, the cavity is assumed to be spherically symmetric and characterized by four different altitude profiles of conductivity $\sigma(z)$: (1) an ideal, free space cavity with $\sigma(z) = 0$; (2) a single-exponential profile with a perturbation [Sentman, 1983], $\sigma(z) = \sigma_0 \exp[\frac{z}{\xi_0} + 2.303\beta \exp - (\frac{z-z_0}{a})^2]$ S/m, where $\sigma_0 = 10^{-16}$ S/m, $\xi_0 = 3.1$ km, a and z_0 indicate the center altitude and width of the perturbation, respectively, and the parameter β describes the amplitude of the perturbation in powers of ten about its unperturbed value; (3) a "knee" profile [e.g., Mushtak and Williams, 2002], $\sigma(z) = \sigma_{kn} \exp [(z - h_{kn})/\xi_b]$ for $z < h_{kn}$ and $\sigma(z) = \sigma_{kn} \exp [(z - h_{kn})/\xi_a]$ for $z \geq h_{kn}$, where $h_{kn} = 55$ km, $\xi_a = 2.9$ km, $\xi_b = 8.3$ km, and $\sigma_{kn} = 2 \pi f_{kn} \epsilon_0 = 5.56 \times 10^{-10}$ S/m assuming $f_{kn} = 10$ Hz; and (4) a two-exponential profile [Greifinger and Greifinger, 1978; Sentman, 1990, 1996; Mushtak and Williams, 2002], which is based on a division

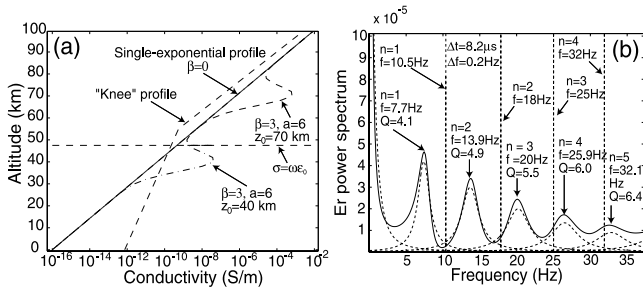


Figure 1. (a) Model conductivity profiles; (b) the E_r power spectrum in the ideal cavity (vertical dashed lines) and a cavity with “knee” conductivity profile (solid line).

of atmosphere into lower (from ground and up to ~60–70 km) and upper (above ~60–70 km) layers with conductivity profiles $\sigma(z) = \sigma(h_1) \exp[(z - h_1)/\xi_1]$ and $\sigma(z) = \sigma(h_2) \exp[(z - h_2)/\xi_2]$, respectively, where $h_1 = 50$ km, $\xi_1 = 5$ km, $h_2 = 93.5$ km, $\xi_2 = 5$ km, $\sigma(h_1) = 2\pi f_0 \epsilon_0 = 4.44 \times 10^{-10}$ S/m, and $\sigma(h_2) = 1/8\mu_0\pi f_0 \xi_1^2 = 1.58 \times 10^{-4}$ S/m assuming $f_0 = 8$ Hz. The “knee” profile and the single-exponential profile with two exemplary perturbations are illustrated in Figure 1a. The specific choice of parameters for profiles 2–4 is motivated by the availability of solutions of related problems [e.g., Sentman, 1983; Mushtak and Williams, 2002], against which the FDTD results presented in this paper are compared.

3. Results

[6] Figure 1b illustrates the E_r power spectra obtained at 18°N 0°E, about 2000 km from the source, with FDTD model for an ideal cavity and a cavity with the “knee” profile. The first four resonance frequencies of the ideal cavity in Figure 1b are within 3% of the respective values 10.52, 18.2, 25.76 and 33.26 Hz obtained from the analytical solution [Schumann, 1952; Roldugin et al., 2001]: $f_n = \frac{c}{2\pi R_E} \sqrt{n(n+1)(1-h/R_E)}$, where c is the speed of light in free space. The f_n and Q_n values shown in Figure 1b for the “knee” profile, are also included in Table 1 along with the reference theoretical data for the same profile from [Ishaq and Jones, 1977], which have been discussed recently in the context of different analytical SR models by Mushtak and Williams [2002]. The FDTD and Ishaq and Jones [1977] results agree within 3% in terms of both f_n and Q_n values for the first five modes considered. The dashed lines in Figure 1b illustrate the employed least squares Lorentzian fits used to determine f_n and Q_n for the “knee” model case. The f_n and Q_n values in Figure 1b agree with those measured at other receivers (not shown), except for the 90°N 0°E case, which corresponds to the null for the odd number modes. The quasi-DC component in Figure 1b is due to the static charges deposited by the model lightning current in the vicinity of the conducting Earth sphere. The discussion of the DC component is beyond the scope of the present paper and we only note here that in addition to other factors (i.e., distance to the source, atmospheric conductivity, etc) its representation in the frequency domain is generally a function of the total sampling time.

[7] Open circles in Figures 2a and 2b report results on variation of f_1 and Q_1 values, respectively, as a function of altitude z_0 of the perturbation of the single-exponential

conductivity profile. Results obtained by Sentman [1983] using mode theory for the same profiles are also shown in Figures 2a and 2b by solid lines. The FDTD results appear to be in good agreement with results of Sentman [1983]. Figure 2a, in particular, indicates that z_0 values below ~60 km lead to a depressed eigenfrequency, while those above ~60 km lead to increase in the frequency. These results can be interpreted following ideas presented by Sentman [1983] based on introduction of a reference boundary defined by a condition $\omega = \sigma/\epsilon_0$ (shown in Figure 1a assuming $\omega = 2\pi \times 8$ Hz) dividing the atmosphere into two altitude regions dominated by displacement (below it) and conduction (above it) currents. Below this boundary the electric field is predominantly vertical and its behavior is similar to that in loss-less free space resonator, while above it the vertical component of the field drops exponentially due to large conductivity, with the field becoming virtually parallel to the Earth’s surface above 80 km [Sentman, 1983] as illustrated in Figure 3a. Figure 3a reports altitude profiles of the global averages of the vertical E_r and tangential E_θ components obtained using FDTD model for the unperturbed single-exponential profile. These distributions are obtained by global averaging of the peak powers (for the 1st SR mode) at each altitude grid point. Sentman [1983] states: “At low altitudes, the atmosphere is a poor conductor, so increasing the conductivity there increases the dissipation with the consequence of lowering the eigenfrequency of the mode. At high altitudes the atmosphere is already a very good, but not perfect, conductor, so increasing the conductivity there decreases the dissipation by making the ionosphere a more perfect reflecting surface, thereby raising the eigenfrequency”. These frequency variation aspects will be further discussed in Section 4 with relation to recent experiments.

[8] The two-exponential conductivity profile has played an important role in the development of analytical theory of SR [e.g., Sentman, 1990, 1996; Mushtak and Williams, 2002]. Results of FDTD modeling using this profile with parameters introduced in Section 2 (providing a good agreement with experimental observations of f_n values in a real cavity [e.g., Mushtak and Williams, 2002]) are shown in Table 1 along with the corresponding f_n and Q_n values from Table 4 of Mushtak and Williams [2002] calculated using a two-exponential model. The results of FDTD model agree with the two-exponential analytical model very well (to within 3%) in terms of both f_n and Q_n values. The two-exponential conductivity model leads to a very flat frequency dependence of Q factor, and generally fails to properly reproduce the Q values observed experimentally and

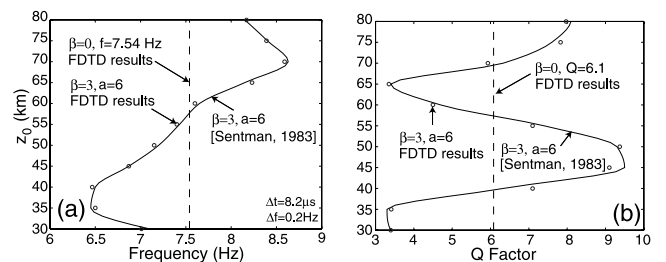


Figure 2. The frequency (a) and Q value (b) shifts with the conductivity perturbation at different altitude.

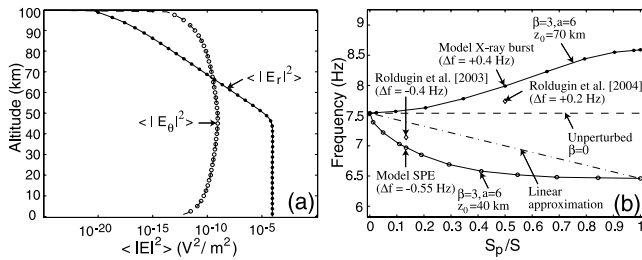


Figure 3. (a) The global averages of the E_r and E_θ components; (b) the first mode SR frequency as a function of effective perturbed area S_p/S in the Earth-ionosphere cavity.

obtained for the “knee” model (see Table 1 and discussion by *Mushtak and Williams* [2002]).

[9] A true 3-D nature of the FDTD model can be explored by considering non-uniform model cavities. Figure 3b documents variations of the first SR frequency f_1 as a function of the spherical area S_p covered with a conductivity perturbation (normalized by the total Earth’s area S), assuming the laterally uniform single-exponential ambient conductivity profile shown in Figure 1a. We consider two conductivity perturbation profiles corresponding to $z_0 = 40$ km and $z_0 = 70$ km (Figure 1a). The area S_p of the perturbation corresponding to $z_0 = 40$ km is assumed to consist of two azimuthally symmetric segments centered at south and north poles and to increase with latitude such that $S_p/S = 1$ when two segments merge in the equatorial plane. The corresponding results are shown by open circles connected by a solid line in Figure 3b. The area S_p of the perturbation corresponding to $z_0 = 70$ km is assumed to have similar geometry to the $z_0 = 40$ km case, but to grow from the north pole only, with the $S_p/S = 1$, in this case, corresponding to the perturbed area reaching the south pole, and $S_p/S = 0.5$ to a perturbation extending from the north pole to the equatorial plane and effectively covering half of the Earth surface. The corresponding results are shown by stars connected by a solid line in Figure 3b. A dash-dot line in Figure 3b illustrates a linear approximation, which is commonly employed in the existing literature in order to estimate changes in observed SR frequency f_{obs} using uniform models [e.g., *Schlegel and Füllekrug*, 1999; *Roldugin et al.*, 2001, 2003]: $f_{obs} = f_u (S - S_p)/S + f_p S_p/S$, where f_u and f_p correspond to uniform spherically symmetric cavity solutions with unperturbed and perturbed conductivity profiles, respectively. Results in Figure 3b indicate that a factor of 2–3 errors in Δf values are possible due to this approximation for small S_p/S around 0.1

(typically $S_p/S = 0.13$ is used to approximate an area affected by SPEs [*Roldugin et al.*, 2001, 2003]).

4. Discussion

[10] *Mushtak and Williams* [2002] have recently discussed different laterally uniform conductivity models of the Earth-ionosphere cavity and noted that the single-exponential model and the two-exponential model (using the same scale height for both conductivity segments) discussed earlier in our paper are not capable of reproducing realistic variation of Q_n values with frequency. This aspect was attributed by *Mushtak and Williams* [2002] to the existence of two distinct altitude layers of energy dissipation within the lower ionosphere and a physical change between the ion-dominated and electron-dominated conductivity as a function of altitude, which has a “knee”-like shape when conductivity is plotted as a function of altitude on a logarithmic scale. *Mushtak and Williams* [2002] argued that the observed increase in Q_n values with frequency can be traced in the case of “knee”-like conductivity to an upward migration of the lower dissipation layer through the “knee” region leading to decrease in scale height of conductivity and increase in Q_n values. The FDTD results presented in Table 1 support ideas of *Mushtak and Williams* [2002] indicating that the “knee” model is indeed capable of simultaneous reproduction of the realistic f_n values and Q_n factors as a function of frequency, and that these parameters can not be reproduced with single scale height models (i.e., single- or two-exponential profiles discussed in previous sections). The f_n and Q_n values calculated with FDTD model for the unperturbed single-exponential profile are included in Table 1. These values are in good agreement with results of *Sentman* [1983]. As expected, the Q factors remained flat with the frequency. We have performed series of additional numerical experiments in which we varied the scale height of the single-exponential profile. The Q factors increased with the reduction of the scale height, but remained flat as a function of frequency, reaching very high values as system approached the ideal cavity regime.

[11] The SR frequencies are known to undergo daily and seasonal variations of approximately ± 0.5 Hz [e.g., *Satori*, 1996; *Price and Melnikov*, 2004]. Besides these periodic and repeatable variations the SR frequencies can also vary due to relatively transient ionization events in the lower ionosphere. The most pronounced examples of these include SPEs, which can produce ionization in polar cap regions down to 30–40 km altitudes [e.g., *Roldugin et al.*,

Table 1. Comparison of the Eigenfrequencies and Q Factors in the Different Conductivity Models

Mode Number (n)	Reference Model [<i>Ishaq and Jones</i> , 1977]		FDTD With “Knee” Profile		Two-Exponential Model [<i>Mushtak and Williams</i> , 2002, Table 4]		FDTD With Two-Exponential Profile		FDTD With Single-Exponential Profile	
	f_n	Q_n	f_n	Q_n	f_n	Q_n	f_n	Q_n	f_n	Q_n
1	7.7	4.1	7.7	4.1	7.7	4.2	7.6	4.2	7.54	6.1
2	14.0	4.9	13.9	4.9	13.9	4.3	13.6	4.1	13.4	6.2
3	20.2	5.4	20.0	5.5	20.2	4.3	19.7	4.2	19.2	6.3
4	26.5	5.9	25.9	6.0	26.6	4.4	25.8	4.4	24.8	6.4
5	32.8	6.3	32.1	6.4	33.1	4.4	32.0	4.6	30.4	6.3

2003, and references therein], and solar X-ray bursts, typically producing an additional ionization at altitudes above 60–70 km, which lasts less than 1 hour, but covers an entire Earth's hemisphere [e.g., *Roldugin et al.*, 2004, and referenced therein].

[12] *Schlegel and Füllekrug* [1999] studied daily averaged values of the first mode SR frequency during nine SPEs and found the frequency increases by 0.04–0.14 Hz, in good correlation with observed integral solar proton fluxes with energies >1 MeV. *Roldugin et al.* [2001, 2003] considered most energetic components of SPEs (protons with energies >100 MeV) lasting only several hours and reported the time resolved (the resonance frequency was determined for each of 5 min intervals) decreases of the first mode frequency by ~0.15–0.4 Hz. Given the fact that solar X-ray bursts typically precede proton precipitation events on the same day and that these two types of phenomena are expected to produce opposite effects on eigenfrequencies (see below), the contradiction between the above two results is likely related to differences in time scales chosen for the analysis [*Roldugin et al.*, 2001, 2003]. In accordance with the arguments of *Sentman* [1983] the high energy protons producing conductivity enhancement at altitudes 30–40 km (qualitatively corresponding to profile $z_0 = 40$ km in Figure 1a) are expected to lead to the SR frequency decreases due to the increased dissipation at lower altitudes. Figure 3b includes the $\Delta f = -0.4$ Hz experimental result at $S_p/S = 0.13$ reported by *Roldugin et al.* [2003]. The close agreement between the model and observations for this case is more or less coincidental, given the model nature of the conductivity profiles used, however, the modeling correctly reflects the general trend of reduction of the eigenfrequency due to the ionization at lower altitudes in accordance with the physical arguments discussed above.

[13] *Roldugin et al.* [2004] reported the first resonance frequency increases by 0.2 Hz (shown in Figure 3b at $S_p/S = 0.5$) during some very intense solar X-ray bursts. In accordance with arguments of *Sentman* [1983] discussed in Section 3 a conductivity enhancement at altitudes above 60–70 km in association with solar X-ray bursts is expected to lead to an increased eigenfrequency by making the upper boundary in the cavity a better conductor. Results presented in Figure 3b for $z_0 = 70$ km qualitatively support this argument in agreement with observations of *Roldugin et al.* [2004].

[14] **Acknowledgment.** This research was supported by NSF ATM-0134838 grant to Penn State University.

References

- Adve, R. S., T. K. Sarkar, S. M. Rao, E. K. Miller, and D. R. Pflug (1997), Application of the Cauchy method for extrapolating/interpolating narrow-band system responses, *IEEE Trans. Microwave Theory Tech.*, *45*, 837.
- Berenger, J. P. (2002), FDTD computation of VLF-LF propagation in the Earth-ionosphere waveguide, *Ann. Telecommun.*, *57*, 1059.
- Cummer, S. A. (2000), Modeling electromagnetic propagation in the Earth-ionosphere waveguide, *IEEE Trans. Antennas Propag.*, *48*, 1420.
- Füllekrug, M. (1995), Schumann-resonances in magnetic-field components, *J. Atmos. Terr. Phys.*, *57*, 479.

- Greifinger, C., and P. Greifinger (1978), Approximate method for determining ELF eigenvalues in the Earth-ionosphere cavity, *Radio Sci.*, *13*, 831.
- Heckman, S. J., E. Williams, and B. Boldi (1998), Total global lightning inferred from Schumann resonance measurements, *J. Geophys. Res.*, *103*, 31,775.
- Hildebrand, F. B. (1956), *Introduction to Numerical Analysis*, McGraw-Hill, New York.
- Ishaq, M., and D. L. Jones (1977), Method of obtaining radiowave propagation parameters for the Earth-ionosphere duct at ELF, *Electron. Lett.*, *13*, 254.
- Mushtak, V. C., and E. Williams (2002), ELF propagation parameters for uniform models of the Earth-ionosphere waveguide, *J. Atmos. Sol. Terr. Phys.*, *64*, 1989.
- Otsuyama, T., D. Sakuma, and M. Hayakawa (2003), FDTD analysis of ELF wave propagation and Schumann resonances for a subionospheric waveguide model, *Radio Sci.*, *38*(6), 1103, doi:10.1029/2002RS002752.
- Pasko, V. P., U. S. Inan, T. F. Bell, and S. C. Reising (1998), Mechanism of ELF radiation from sprites, *Geophys. Res. Lett.*, *25*, 3493.
- Price, C., and A. Melnikov (2004), Diurnal, seasonal and inter-annual variations of the Schumann resonance parameters, *J. Atmos. Sol. Terr. Phys.*, *66*, 1179.
- Roldugin, V. C., Y. P. Maltsev, G. A. Petrova, and A. N. Vasiljev (2001), Decrease of the first Schumann resonance frequency during solar proton events, *J. Geophys. Res.*, *106*, 18,555.
- Roldugin, V. C., Y. P. Maltsev, A. N. Vasiljev, A. V. Shvets, and A. P. Nikolaenko (2003), Changes of Schumann resonance parameters during the solar proton event of 14 July 2000, *J. Geophys. Res.*, *108*(A3), 1103, doi:10.1029/2002JA009495.
- Roldugin, V. C., Y. P. Maltsev, A. N. Vasiljev, A. Y. Schokotov, and G. G. Belyajev (2004), Schumann resonance frequency increase during solar X-ray bursts, *J. Geophys. Res.*, *109*, A01216, doi:10.1029/2003JA010019.
- Sato, M., and H. Fukunishi (2003), Global sprite occurrence locations and rates derived from triangulation of transient Schumann resonance events, *Geophys. Res. Lett.*, *30*, 1859, doi:10.1029/2003GL017291.
- Satori, G. (1996), Monitoring Schumann resonances—II. Daily and seasonal frequency variations, *J. Atmos. Terr. Phys.*, *58*(13), 1483.
- Schlegel, K., and M. Füllekrug (1999), Schumann resonance parameter changes during high-energy particle precipitation, *J. Geophys. Res.*, *104*, 10,111.
- Schumann, W. O. (1952), Über die strahlungslosen eigenschwingungen einer leitenden Kugel die von einer Luftschicht und einer Ionosphärenhülle umgeben ist, *Z. Naturforsch.*, *7a*, 149.
- Sentman, D. D. (1983), Schumann resonance effects of electrical conductivity perturbations in an exponential atmospheric/ionospheric profile, *J. Atmos. Terr. Phys.*, *45*, 55.
- Sentman, D. D. (1987), Magnetic elliptic polarization of Schumann resonances, *Radio Sci.*, *22*, 595.
- Sentman, D. D. (1990), Approximate Schumann resonance parameters for a 2-scale-height ionosphere, *J. Atmos. Terr. Phys.*, *52*, 35.
- Sentman, D. D. (1996), Schumann resonance spectra in a two-scale-height Earth-ionosphere cavity, *J. Geophys. Res.*, *101*, 9479.
- Simpson, J. J., and A. Taflove (2002), Two-dimensional FDTD model of antipodal ELF propagation and Schumann resonance of the Earth, *Antennas Wireless Propag. Lett.*, *1*, 53.
- Simpson, J. J., and A. Taflove (2004), Three-dimensional FDTD modeling of impulsive ELF propagation about the earth-sphere, *IEEE Trans. Antennas Propag.*, *52*, 443.
- Taflove, A., and S. C. Hagness (2000), *Computational Electrodynamics: The Finite-Difference Time-Domain Method*, Artech House, Norwood, Mass.
- Thevenot, M., J. P. Berenger, T. Monediere, and F. Jecko (1999), A FDTD scheme for the computation of VLF-LF propagation in the anisotropic Earth-ionosphere waveguide, *Ann. Telecommun.*, *54*, 297.
- Williams, E. R. (1992), The Schumann resonance—A global tropical thermometer, *Science*, *256*, 1184.
- Yang, H., and V. P. Pasko (2003), Three-dimensional FDTD Modeling of Earth-ionosphere cavity resonances, *Eos Trans. AGU*, *84*(46), Fall Meet. Suppl., Abstract AE42A-0796.

V. P. Pasko and H. Yang, CSSL Laboratory, Pennsylvania State University, 211B EE East, University Park, PA 16802, USA. (vpasko@psu.edu; hxy149@psu.edu)